

The Effect of Calcination Temperature on the Electrochemical Performance of ZnO Coated LiMn₂O₄/MWCNT Nanocomposite Cathodes

A. AKBULUT^{a,*}, T. CETINKAYA^b, M.O. GULER^b AND H. AKBULUT^b

^aSakarya University, Dept. of Environmental Engineering, Esentepe Campus, 54187, Sakarya, Turkey

^bSakarya University, Metallurgy and Materials Engineering, Esentepe Campus, 54187 Sakarya, Turkey

In this study, it is aimed to develop LiMn₂O₄/MWCNT nanocomposite cathode materials by using different calcination temperatures (300, 500, 700 °C). The aim of using MWCNTs in the active material is to overcome poor conductivity and to increase stability of the electrodes during charging and discharging. The nanocomposites were produced by sol-gel method, which allows producing very fine particle size of LiMn₂O₄. LiMn₂O₄ and LiMn₂O₄/MWCNT were uniformly coated on an Al-foil to obtain 500 μm thicknesses with a specific amount of binder and conducting agent. The surfaces of cathodes were coated with ZnO by using magnetron sputtering PVD with a thickness of 10 nm. Coin-type (CR2016) test cells were assembled, directly using the LiMn₂O₄/MWCNTs and surface coated LiMn₂O₄/MWCNTs as anode and a lithium metal foil as the counter electrode.

DOI: [10.12693/APhysPolA.125.331](https://doi.org/10.12693/APhysPolA.125.331)

PACS: 82.47.Aa, 81.05.Mh, 81.20.Fw, 68.47.Gh

1. Introduction

In the Li-ion batteries, LiCoO₂, LiNiO₂, LiFePO₄ and LiMn₂O₄ are considered most important cathode materials [1, 2]. Unlike LiCoO₂, LiNiO₂ and LiFePO₄, spinel LiMn₂O₄ has become promising energy source and does not contain heavy metals to dispose after usage [3].

Furthermore, LiMn₂O₄ batteries have advantages as their low cost, abundant resource, easy preparation [4]. Despite the advantages, LiMn₂O₄ batteries suffer from capacity fading which restricts their commercial usage. This capacity fading results from: (I) dissolution of Mn²⁺, (II) the Jahn–Teller distortion, and (III) decomposition of electrolyte solution on the electrode. Mn²⁺ ion dissolution into the electrolyte, which occurs because of the reaction in the interface between electrolyte and electrode, is considered a main source of capacity fading [4, 5]. To address disadvantages, doping different cations into spinel LiMn₂O₄ [6], surface treatment of the cathode with pure stable metals and metal oxides are most promising methods [7–9]. Multiwalled carbon nanotubes (MWCNTs) have unique one-dimensional tubular structure, high electrical conductivity, and large surface area, and have been considered an ideal nanomaterial to functionalize other materials for applications in energy conversion and storage. Therefore, electrical conductivity of the LiMn₂O₄ battery increases while decreasing the charging resistance. Hybrid nanostructures composed of MWCNTs, and active materials possess not only the inherent properties of nanocrystals and MWCNTs acting alone, but also additional, unique properties that arise from the electrical and thermal interactions between them [10].

In this study, it is aimed to determine calcination temperature and ZnO surface coating effects on the elec-

trochemical properties in the LiMn₂O₄ and LiMn₂O₄/MWCNT nanocomposite by using citric acid sol-gel method. Although there were several studies in the open literature, applying cathode surface coating with metal oxide and gold, there is no comprehensive study to show both surface coating and MWCNTs reinforcement effect together.

2. Experiment details

The LiMn₂O₄ powders were produced by using a well-known sol-gel method. The precursor materials were high-purity Mn(CH₃COO)₂·4H₂O, LiCH₃COO·2H₂O and citric acid as a chelating agent. These precursors were dissolved in distilled water, and ammonia added to maintain pH between 7 and 10. Then the obtained solution was heated with vigorous stirring to remove excess ammonia and water. The resultant gel was dried at 120 °C for 10 h and calcinated at the temperatures of 300 °C, 500 °C and 700 °C for 24 h in air to determine the effect of calcination temperature on nanocrystalline structure and cell performance. The nanocomposites of LiMn₂O₄ reinforced with 5 wt% MWCNT was prepared by mechanical alloying. MWCNTs and LiMn₂O₄ powders was placed in 80 ml stainless steel mixing jars containing steel milling balls of 10 mm diameter (giving an initial ball-to-powder weight ratio (BPR) = 15:1). The jars were agitated using a high-energy planetary ball mill (Fritsch Pulverisette F7) at 500 rpm for milling time of 1 h. For electrode preparation, 70 wt% LiMn₂O₄ powders were mixed with 20 wt% acetylene black (conducting agent), and 10 wt% polyvinylidene fluoride (binder-PVDF). Excess was 1-methyl-2-pyrrolidone (NMP). The slurry was uniformly coated on an Al-foil to obtain 500 μm thicknesses. The surfaces of some selected bare cathodes and nanocomposites were coated

with ZnO by magnetron sputtering method with thickness of 10 nm.

A Rigaku (D/MAX/2200)X-ray diffraction (XRD) with a grazing incidence attachment and Cu K_{α} radiation was used. The diffraction patterns were registered in the step scan mode, with a beam incidence angle of 0.5° , and recorded at 2° (2θ) steps with a constant time of 1 min per step. Scanning electron microscopy (SEM) (JEOL 6060LV) has been used to determine morphologies of the nanocomposite electrodes. Coin-type (CR2016) test cells were assembled in an argon-filled glove box, directly using the LiMn_2O_4 and $\text{LiMn}_2\text{O}_4/\text{MWCNTs}$. The cells were cyclically tested on a MTI-BST8 battery tester using 0.4 C over a voltage range of 3.0–4.3 V. All tests were performed at room temperature (25°C). The electrochemical impedance spectroscopy (EIS) was carried out by applying an ac voltage of 10 mV over the frequency range from 1 Hz to 1000 kHz (Gamry Instrument Version 5.67).

3. Results and discussions

Figure 1 presents LiMn_2O_4 powders surface morphology at different temperatures (a, c, d) and nanocomposite of $\text{LiMn}_2\text{O}_4/\text{MWCNT}$ calcinated at 300°C (b). 500°C and 700°C calcinated reinforced powders are not shown because the microstructure of all MWCNT reinforced samples after grinding is very similar to each other. It can be seen from the SEM images that LiMn_2O_4 powders are fine particles and have homogeneous morphology. SEM images indicate that grain sizes of LiMn_2O_4 powders increase with increasing calcination temperatures. However, because of using citric acid sol-gel method, LiMn_2O_4 powders still have small particle size even at calcination temperature of 700°C . This was caused from faster growing speed and agglomerated areas turn into large particles with temperature [11, 12]. MWCNTs, marked in Fig. 1b, were dispersed into LiMn_2O_4 nanopowders as a network in all reinforced powders.

Figure 2 shows discharge capacities of the bare LiMn_2O_4 , $\text{LiMn}_2\text{O}_4/\text{MWCNT}$ electrodes after calcination at 300, 500, and 700°C and cyclically tested at room temperature. The electrodes calcinated at 300 and 500°C show similar initial capacities and the capacity fading rates (Fig. 2a and b). The bare LiMn_2O_4 shows high initial capacity but the cell performance exhibits very sharp decrease in the capacity with increasing cycle number. Coating of LiMn_2O_4 electrode surfaces with magnetron sputtering yields higher discharge capacities for the initial cycles and also prevented the decrease of capacity with increasing cycles.

Introducing 5 wt% MWCNTs into LiMn_2O_4 results to increase both initial capacity and capacity retention with increasing cycle for all calcination temperature conditions. When the LiMn_2O_4 was reinforced with MWCNTs and coated with ZnO, produced excellent capacity retentions. In these composites, the capacity retention was

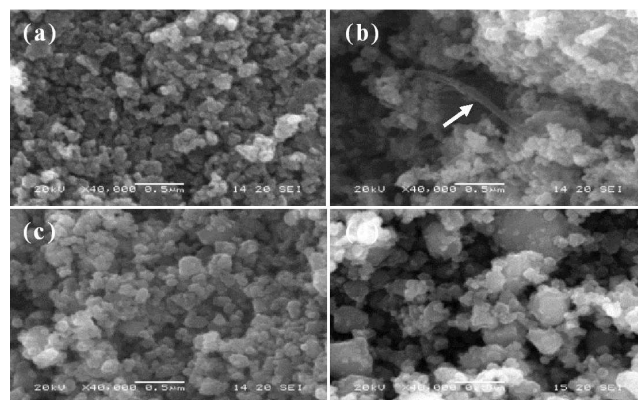


Fig. 1. SEM photographs of (a) 300°C calcinated LiMn_2O_4 , (b) 300°C calcinated $\text{LiMn}_2\text{O}_4/\text{MWCNT}$ nanocomposite, (c) 500°C , and (d) 700°C calcinated LiMn_2O_4 nanopowders after grinding.

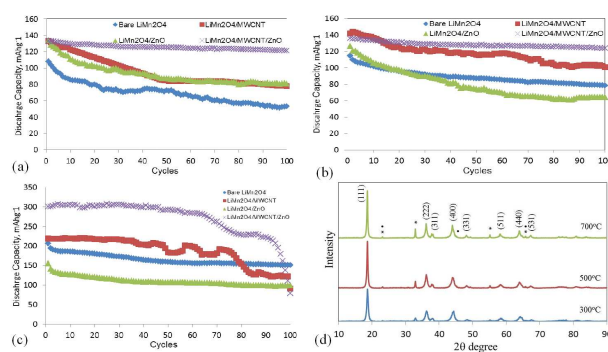


Fig. 2. Discharge capacity versus cycle number for LiMn_2O_4 and nanocomposites calcinated at (a) 300°C , (b) 500°C , (c) 700°C , and (d) XRD patterns of nanocomposites calcinated at three different temperatures (■ LiMn_2O_4 , * Mn_2O_3 , • Li_2MnO_3).

calculated as 95% even at the 100th cycle. This high capacity retention is attributed to the combined effects of high conductivity emanated from MWCNTs and surface coating with ZnO, which prevents dissolution of the Mn into the electrolyte.

However, the electrodes calcinated at 700°C show dissimilar characteristics depending on the increased amount of Mn_2O_3 and formation of layered LiMn_2O_3 as can also be seen in the XRD analysis. In these electrodes, very high initial discharge capacities were obtained.

For example, the initial capacity of the electrode yielded approximately 300 mAh g^{-1} but showed very high capacity fading after 90th cycle and almost failed in the 100th cycle (Fig. 2c). Theoretically, LiMn_2O_4 has 148 mAh g^{-1} discharge capacity [13]. However, it is believed that increasing the calcination temperature resulted in increase of amount of layered LiMn_2O_3 structure.

In recent years, it was reported that Li-excess layered oxides have a very high discharge capacity, but

have many problems such as voltage instability, capacity fading and slow charge/discharge rate preventing them from commercialization [14]. Increasing discharge capacity and/or cycle number resulted in very high capacity fading in the layered type of the cathode materials.

The XRD analysis of the nanocomposites at three different calcination temperatures is presented in Fig. 2d. Layered Li_2MnO_3 and Mn_2O_3 impurity peaks were observed [15]. XRD peaks of 300°C showed broadening, which indicates smaller grain size and micro stretching [16]. When the calcination temperature is increased to 700°C , XRD peaks showed to have sharpened characteristic, which indicates larger grain size and higher crystallinity [11]. The average dimension of crystallites d was estimated from the linewidths of XRD reflections. It was calculated that grain sizes at 300°C , 500°C , and 700°C LiMn_2O_4 were found approximately 22.13, 23.89, and 29.23 nm, respectively. Lattice parameters calculated from the patterns are found to be 8.569 Å for 300°C LiMn_2O_4 and 8.386 Å both for 500°C and 700°C LiMn_2O_4 . Lattice parameter for LiMn_2O_4 was reported as 8.206–8.251 Å in literature [17]. Increasing lattice constant can be attributed to Mn^{4+} ion transitions to Mn^{3+} in high spinstate.

Addition of 5 wt% MWCNT to LiMn_2O_4 nanopowders did not show significant change on grain size and lattice parameter at 300°C . But, for higher calcination temperatures, grain size and lattice parameter values are differed. 5 wt% MWCNT reinforced powders grain size were calculated and found to be 29.23 nm and 38.22 nm at 500°C and 700°C calcination temperatures, respectively. For 500°C and 700°C , MWCNT addition decreased lattice parameters to 8.23 and 8.24, respectively. The reason of decrease in the lattice parameter is increase

in total atom or ions ratio in the surface when compared with the total ions or ions in the crystal [18].

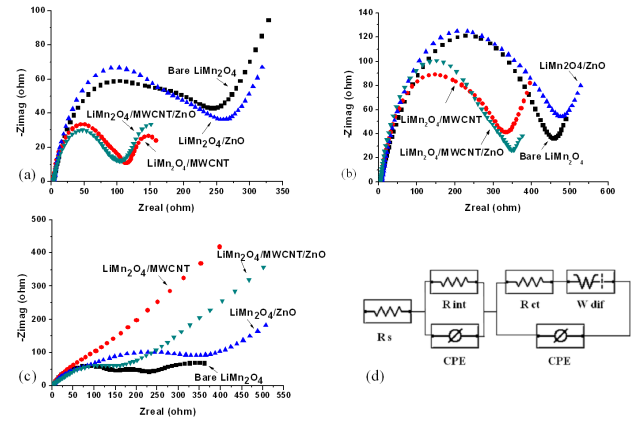


Fig. 3. EIS spectra for LiMn_2O_4 and nanocomposites calcinated at (a) 300°C , (b) 500°C , (c) 700°C , and (d) the equivalent circuitmodel.

In Fig. 3, the Nyquist plots, and the equivalent circuit model is presented. On this circuit, R_s is the resistance associated with the electrolyte and cell component, R_{int} is the resistance of any film formation on the cathode surface (first HF semicircle), R_{ct} is the charge-transfer resistance of the electrode reaction with lithium ions (middle frequency semicircle), and W_{dif} is the resistance of the lithium ion diffusion to the electrode (low frequency semicircle) [19]. The R_{ct} results are presented in Table before testing the electrochemical performances.

Electrochemical impedance parameters of calculated from equivalent circuitmodel.

TABLE

Samples	R_{ct}	Samples	R_{ct}	Samples	R_{ct}
$300^\circ\text{C}/\text{bare}$	448.1	$500^\circ\text{C}/\text{bare}$	115	$700^\circ\text{C}/\text{bare}$	146
$300^\circ\text{C}/\text{MWCNT}$	190.3	$500^\circ\text{C}/\text{MWCNT}$	31.01	$700^\circ\text{C}/\text{MWCNT}$	108.4
$300^\circ\text{C}/\text{ZnO}$	339	$500^\circ\text{C}/\text{ZnO}$	129	$700^\circ\text{C}/\text{ZnO}$	296.8
$300^\circ\text{C}/\text{MWCNT ZnO}$	266.7	$500^\circ\text{C}/\text{MWCNT ZnO}$	35.15	$700^\circ\text{C}/\text{MWCNT ZnO}$	140

It can be seen from Fig. 3 that for all the calcination temperatures condition, introducing MWCNT into LiMn_2O_4 seems to be very effective to decrease the charge transfer resistance. This is attributed to the increased conductivity and amount of Li ions absorption emanated from MWCNTs [10].

It is well known that the semicircle corresponding to the passivation film formed by the reaction between the oxide and electrolyte [20]. The decrease of the diameter in the semicircle is seen for all the nanocomposite electrodes, produced by introducing MWCNTs.

Literature about EIS reports that a circle at the high-to-middle frequency semicircle represents the resistance for the Li-ions migration through the EIS layer and film capacitance. Another semicircle at the low-frequency semicircle is related to charge transfer resistance and interfacial capacitance between the electrode and electrolyte interface, and the sloping straight line at very low frequency corresponds to the Li-ions diffusion in the bulk materials. The intercept of the high-frequency semicircle on the real axis (z real axis) represents resistance contribution coming from the electrolyte solution [21].

According to the EIS results obtained in this study, they evidenced that coating the surfaces of the nanocomposite electrodes with ZnO magnetron sputtering resulted in a small increase in the charge transfer resistance. This is because coating the surfaces of electrodes causes to increase the surface tension and prevents the electrolyte impregnation at the initial stages. As shown in the discharge capacity results versus the cycle number (Fig. 3), these surface coated electrodes showed higher capacity retention and thus, less capacity fading. Therefore, from the EIS results, it can be concluded that MWCNT addition and coating the electrode surfaces with a 10 nm ZnO provided very attractive results to prevent Mn dissolution into the electrolyte. It can be speculated that the surface coating of ZnO suppressed the formation of passivation on the surface of the LiMn_2O_4 , preventing the electrolyte decomposition which leads to the dissolution of the Mn ion.

4. Conclusions

Citric acid sol-gel method was used to produce LiMn_2O_4 electrodes at 300 °C, 500 °C, and 700 °C calcination temperatures. Introducing 5.0 wt% MWCNT into LiMn_2O_4 increased discharge capacity of the LiMn_2O_4 and as high as 95% capacity retention values were obtained even after 100 cycles. Increasing the calcination temperatures resulted in producing both Li_2MnO_3 and Mn_2O_3 together with spinel LiMn_2O_4 . Since the Li_2MnO_3 has layered structure, the initial discharge capacity was obtained very high (300 mAh g^{-1}) but decreased rapidly by increasing cycle number. ZnO coatings on LiMn_2O_4 /MWCNT nanocomposites with 10 nm thickness increased the discharge capacity and provided excellent capacity retention. EIS measurements showed that MWCNT addition provides the decrease in charge transfer resistance.

Acknowledgments

The authors thank the Scientific and Technological Research Council of Turkey (TÜBİTAK) for their financial support under the contract number of 111M021.

References

- [1] B. Xu, D. Qian, Z. Wang, Y.S. Meng, *Mater. Sci. Eng. R* **73**, 51 (2012).
- [2] M.G. Kim, J. Cho, *Adv. Funct. Mater.* **19**, 1497 (2009).

- [3] H. Sun, Y. Chen, C. Xu, D. Zhu, L. Huang, *J. Solid State Electrochem.* **16**, 1247 (2012).
- [4] W. Tang, L. Liu, Y. Zhu, H. Sun, Y. Wu, K. Zhu, *Energy Environ. Sci.* **5**, 6909 (2012).
- [5] Q. Liu, Sh. Wang, H. Tan, Z. Yang, J. Zeng, *Energies* **6**, 1718 (2013).
- [6] H.L. Li, S.J. Bao, Y.Y. Liang, W.J. Zhou, B.L. He, *J. Colloid Interface Sci.* **300**, 633 (2006).
- [7] H. Şahan, H. Göktepe,Ş. Patat, *J. Mater. Sci. Technol.* **27**, 415 (2011).
- [8] M. Prabu, M.V. Reddy, S. Selvasekarapandian, S. Admas, K.P. Loh, G.V. Subba Rao, B.V.R. Chowdari, *J. Electrochem. Soc.* **160**, A3144 (2013).
- [9] T.F. Yi, Y.R. Zhu, X.D. Zhu, J. Shu, C.B. Yue, A.N. Zhou, *Ionics* **15**, 779 (2009).
- [10] X.M. Liu, Z.D. Huang, S. Oh, P.C. Ma, P.C.H. Chan, G.K. Vedam, K. Kang, J.K. Kim, *J. Power Sources* **195**, 4290 (2010).
- [11] Y.K. Sun, I.-H. Oh, K.Y. Kim, *Ind. Eng. Chem. Res.* **36**, 4839 (1997).
- [12] M.W. Wu, X.H. Li, Z.B. Xiao, J. Liu, W.B. Yan, M.Y. Ma, *Mater. Chem. Phys.* **84**, 182 (2004).
- [13] M.B. Sassin, S.G. Greenbaum, P.E. Stallworth, A.N. Mansour, B.P. Hahn, K.A. Pettigrew, D.R. Rolison, J.W. Long, *J. Mater. Chem. A* **1**, 2431 (2013).
- [14] N. Yabuuchi, K. Yoshii, S.T. Myung, I. Nakai, S. Komaba, *J. Am. Chem. Soc.* **133**, 4404 (2011).
- [15] B.J. Hwang, R. Santhanam, D.G. Liu, *J. Power Sources* **97-98**, 443 (2001).
- [16] M. Alaf, D. Gultekin, H. Akbulut, *Appl. Surf. Sci.* **275**, 244 (2013).
- [17] M. Michalska, L. Lipinska, R. Diduszko, M. Mazurkiewicz, A. Malolepszy, L. Stobinski, K.J. Kurzydowski, *Phys. Status Solidi C* **7-8**, 2538 (2011).
- [18] N. Kamarulzaman, R. Yusoff, N. Kamarudin, N.H. Shaari, N.A. Abdul Aziz, M.A. Bustam, N. Blagojevic, M. Elcombe, M. Blackford, M. Avdeev, A.K. Arof, *J. Power Sources* **188**, 274 (2009).
- [19] S. Yang, J. Huo, H. Song, X. Chen, *Electrochim. Acta* **53**, 2238 (2008).
- [20] H. Liu, C. Cheng, Zongqiu, K. Zhang, *Mater. Chem. Phys.* **101**, 276 (2007).
- [21] J. Tu, X.B. Zhao, G.S. Cao, J.P. Tu, T.J. Zhu, *Mater. Lett.* **60**, 3251 (2006).